Laser-generated ultrasound with optical fibres using functionalised carbon nanotube composite coatings

Richard J. Colchester, Charles A. Mosse, Davinder S. Bhachu, Joseph C. Bear, Claire J. Carmalt, Ivan P. Parkin, Bradley E. Treeby, Ioannis Papakonstantinou, and Adrien E. Desjardins

Laser-generated ultrasound with optical fibres using functionalised carbon nanotube composite coatings

Richard J. Colchester,[1,a] Charles A. Mosse,[1] Davinder S. Bhachu,[2] Joseph C. Bear,[2] Claire J. Carmalt,[2] Ivan P. Parkin,[2] Bradley E. Treeby,[1] Ioannis Papakonstantinou,[3] and Adrien E. Desjardins[1]

[1]*Department of Medical Physics and Bioengineering, University College London, Malet Place Engineering Building, London WC1E 6BT, United Kingdom*
[2]*Materials Chemistry Centre, Department of Chemistry, University College London, 20 Gordon Street, London WC1H 0AJ, United Kingdom*
[3]*Department of Electronic and Electrical Engineering, University College London, Roberts Building, London WC1E 7JE, United Kingdom*

Optical ultrasound transducers were created by coating optical fibres with a composite of carbon nanotubes (CNTs) and polydimethylsiloxane (PDMS). Dissolution of CNTs in PDMS to create the composite was facilitated by functionalisation with oleylamine. Composite surfaces were applied to optical fibres using dip coating. Under pulsed laser excitation, ultrasound pressures of 3.6 MPa and 4.5 MPa at the coated end faces were achieved with optical fibre core diameters of 105 and 200 μm, respectively. The results indicate that CNT-PDMS composite coatings on optical fibres could be viable alternatives to electrical ultrasound transducers in miniature ultrasound imaging probes. © *2014 Author(s). All article content, except where otherwise noted, is licensed under a Creative Commons Attribution 3.0 Unported License.* [http://dx.doi.org/10.1063/1.4873678]

Miniature ultrasound imaging probes can provide information about tissue from within the body that is invaluable for guiding minimally invasive procedures. For instance, intravascular ultrasound is used to visualise coronary artery plaque morphology during stent placement.[1] In present generation medical devices, ultrasound is generated electrically, using piezoelectric transducers[2] or capacitive micromachined ultrasonic transducers.[3] Fabrication of broadband electrical transducers with millimetre-scale lateral dimensions and integration into medical devices such as catheters with metre-scale longitudinal dimensions can be challenging and expensive.

Recently, there has been rapid progress with the development of optical ultrasound transducers to address the limitations of their electrical counterparts. Optical ultrasound transducers generate ultrasound with the photoacoustic effect: absorption of light results in heating of the material which produces an increase in pressure and the subsequent emission of ultrasonic waves.[4]

Composite media that include distinct elastomeric and absorbing components have emerged as particularly efficient optical transducers. Several absorbers have been considered, including gold nanostructures,[5] carbon black,[6] graphite,[7,8] graphene,[9] and carbon nanotubes (CNTs).[10] The use of polydimethylsiloxane (PDMS) as an elastic component with a large thermal expansion coefficient was highlighted in several studies.[5,6,10] To achieve micron-scale thicknesses for high-frequency ultrasound generation, spin coating was used to apply thin PDMS layers onto CNTs that were grown onto a substrate.[10] While spin coating is well suited for depositing PDMS across large areas, it is ill-suited to coating the distal ends of optical fibres.[11]

Dip coating is a method that is well suited for creating PDMS layers on thin structures such as optical fibres. As an example, it was used to deposit layers of PDMS with a thickness of 10 μm onto the tapered distal ends of conductive wires to fabricate tips for scanning tunnelling microscopy.[12] However, it can be challenging to uniformly dissolve CNTs into PDMS, or organic solvents of PDMS such as xylene, as Van der Waals forces result in CNT agglomerations that hinder dissolution.[13]

In this study, a method for creating a CNT-PDMS composite solution and applying it to the end faces of optical fibres was developed. The performance of the resulting optical ultrasound transducer was investigated.

Multiwall CNTs with specified dimensions of 6–9 nm × 5 μm (724769, Sigma Aldrich, UK) were functionalised to allow for their dissolution in xylene. Functionalisation was performed with a method based on that described by Majeed *et al.*[13] (Figure 1(a)). In this modified method, 1-pyrenebutyric acid (3.5 mmol) and an excess amount of thionyl chloride were transferred to a 25 ml round bottomed flask and refluxed at 100 °C for 30 min.[14] Unreacted $SOCl_2$ was removed by distillation until dry pyrenebutyryl chloride remained. The solid pyrenebutyryl chloride was dissolved in 5 ml anhydrous tetrahydrofuran (THF). Oleylamine (3.5 mmol) and triethylamine (7.1 mmol) were dissolved in anhydrous THF and added to the pyrenebutyryl chloride solution at 0 °C. The reaction mixture was stirred overnight at room temperature and then dissolved in diethyl ether and washed with copious amounts of water. After washing, the organic layer was extracted and dried over sodium sulphate. Finally, diethyl ether was evaporated and the product was dried *in vacuo* at room temperature. The CNTs

---

[a]Author to whom correspondence should be addressed. Electronic mail: richard.colchester.12@ucl.ac.uk
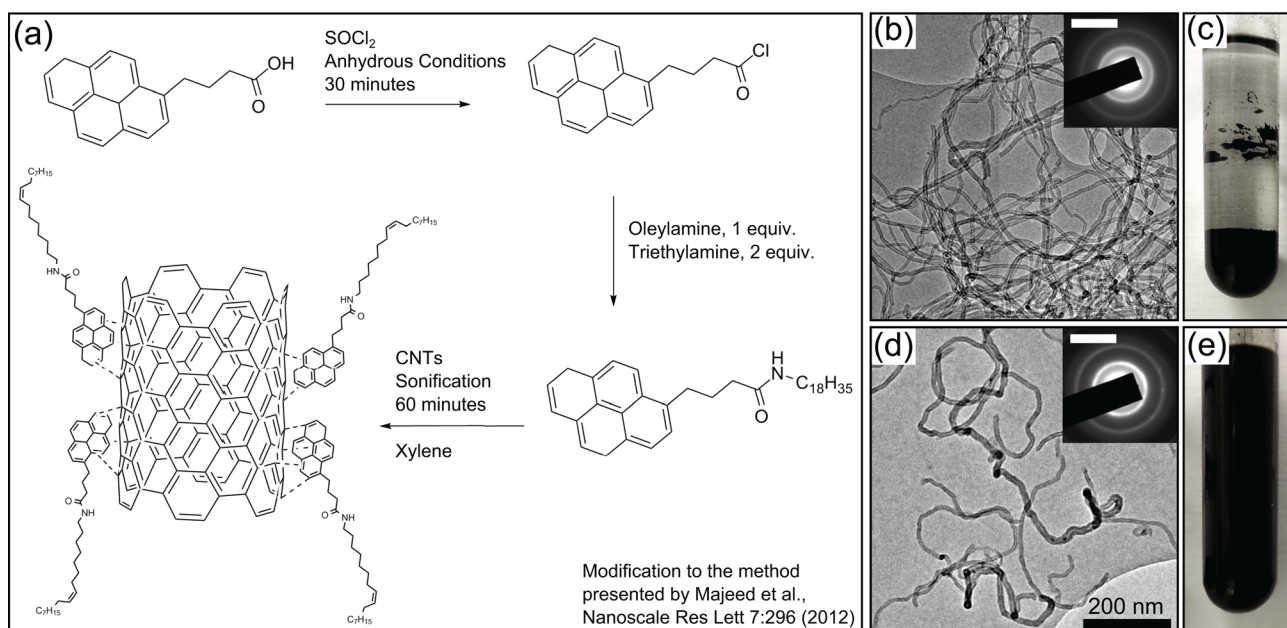
FIG. 1. (a) Schematic of the chemical process to functionalise multi-walled CNTs for their dispersion in xylene. (b) TEM image of non-functionalised CNTs (as received from supplier), with inset showing corresponding SAED pattern indicating carbon (scale bar: $5\,nm^{-1}$). (c) Non-functionalised CNTs in xylene, photographed 10 min after sonication. (d) TEM image of functionalised CNTs, with inset showing corresponding SAED indicating carbon (scale bar: $5\,nm^{-1}$). (e) Functionalised CNTs in xylene, photographed 7 days after sonication.

(300 mg) and oleylamine-functionalised pyrene were dissolved in xylene and sonicated for 1 h. All reactions were carried out under Schlenk conditions.

Transmission electron microscopy (TEM) of the CNT/xylene solution was performed. TEM samples were prepared by drop-casting a suspension of delaminated film in hexane solvent onto a 400 Cu mesh lacy carbon film TEM grid. Selected area electron diffraction (SAED) was also performed.

The CNT-PDMS composite solution for dip coating was created by manually mixing 1.3 ml of the functionalised CNT/xylene solution with 0.5 ml of xylene and 1 g of PDMS (MED-1000, Polymer Systems Technology, Ltd, UK), and subsequently sonicating at 52 W for 10 s and degassing for 2 min.

Dip coating was performed on step-index, silica-core/silica-cladding multimode optical fibres, with core/cladding diameters of $105/125\,\mu m$ and $200/220\,\mu m$, respectively. After mechanical stripping of the buffer layers, the optical fibre tips were cleaved perpendicular to their axes. The cleaved tips were inserted into the dip coating solution, held stationary for 10 s and then withdrawn. Dipping was performed with a motorised stage, with insertion and withdrawal speeds of 2.8 mm/s. After dipping, the coatings were cured for 12 h at $22\,^\circ C$, facing down.

Scanning electron microscopy (SEM) of the coated tips was performed prior to ultrasound generation. Measurements of the optical transmission at 1064 nm were obtained from 5 different optical fibres of each core diameter, using a photodetector and an uncoated optical fibre as a reference.

A fibre coupled Nd:YAG laser with a wavelength 1064 nm, a pulse width of 2 ns, and a repetition rate of 1 kHz (SPOT-10-500-1064, Elforlight, UK) was used to generate ultrasound. Prior to fibre coupling, laser light was transmitted through a variable attenuator that comprised a Brewster window mounted onto a rotating stage. The pulse energies of light delivered to the coatings were $3.6\,\mu J$ and $11.4\,\mu J$ for the $105\,\mu m$-core fibres and the $200\,\mu m$-core fibres, respectively, with corresponding fluences of $41.6\,mJ/cm^2$ and $36.3\,mJ/cm^2$.

Ultrasound pressure measurements were performed with the dip-coated optical fibres positioned in water, facing a hydrophone that was mounted on a motorised positioning system (Precision Acoustics, UK). The hydrophone was a piezoelectric needle hydrophone with a diameter of $75\,\mu m$ (SN 493, Precision Acoustics, UK) and a calibration range of 1–30 MHz. Ultrasound pressure time series were acquired from a spatial plane that was perpendicular to the fibre axis and separated from the distal end of the optical fibre by 2 mm at its closest point. Within this plane, acquisitions were performed in a 6×6 mm planar region centred on the fibre axis, with a grid spacing of $50\,\mu m$.

To estimate the ultrasound pressures produced at the coated end faces of the optical fibres, ultrasound pressure measurements from the two-dimensional region were back-propagated using k-Wave, a numerical simulation toolbox.[15,16] Prior to back propagation, spatial up-sampling to a grid spacing of $25\,\mu m$ was performed to ensure that the simulation could support ultrasound frequencies up to 30 MHz. Temporal down-sampling to a time step of 12.5 ns was performed to improve computational efficiency.

Ultrasound power spectra were measured with a calibrated membrane hydrophone with an active element diameter of $400\,\mu m$ and a frequency response that was nearly flat over the range of 1–30 MHz (Precision Acoustics, UK). The membrane hydrophone faced the coated fibre end face at a distance of 2 mm.

The functionalised CNTs readily dissolved in xylene and formed a stable solution (Figure 1(e)). In comparison, the original, non-functionalised CNTs were largely insoluble
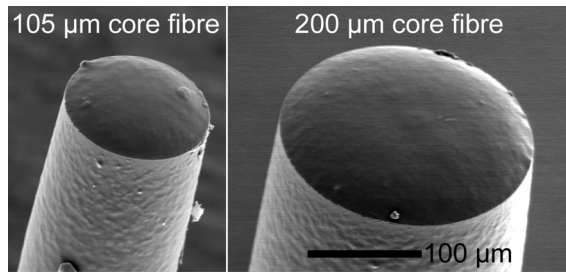
FIG. 2. SEM images of the optical fibres after dip coating with the CNT-PDMS composite.

and sedimentation was apparent within several minutes of mixing (Figure 1(c)). The TEM images suggested that the CNT geometry was unaffected by the functionalisation process; the corresponding selected area electron diffraction images confirmed the presence of carbon (Figures 1(b) and 1(d)).

As seen on the SEM images, the coating surfaces were largely smooth, with a thickness that appeared to decrease slightly from the centre (Figure 2). By visual inspection of these images, the coating thickness was estimated to be less than $20\,\mu m$. The optical transmission at $1064\,nm$ ranged from 13.4% to 15.5% for the $105\,\mu m$-core fibres and from 1.4% to 5.4% for the $200\,\mu m$-core fibres.

At a distance of $2\,mm$ from the optical fibre end faces, the measured ultrasound fields were circularly symmetric (Figures 3(a) and 3(d)), which is consistent with the circular fibre geometry. The temporal profiles were bipolar,

with positive and negative peaks that were equal in magnitude to within 10%. At this distance, the peak positive ultrasound pressures were $0.44\,MPa$ and $0.89\,MPa$ for the optical fibres with core diameters of $105\,\mu m$ and $200\,\mu m$, respectively.

As the fluences approached values that were 30% greater than those used for ultrasound measurements, the peak pressures decreased by approximately 90%. After these decreases were observed, the fluences were not increased further. No damage to the coatings was apparent upon visual inspection with a stereo microscope. After withdrawing the fibres from the water and air-drying them and using normal fluences, no changes in ultrasound pressure measurements were observed.

The back-propagated ultrasound fields at the fibre end faces had peak pressures of $3.6\,MPa$ and $4.5\,MPa$ (Figures 3(c) and 3(f)). Normalised by the fluence, these peak pressures were 0.10 and 0.13 $MPa/(mJ/cm^2)$ for the $105\,\mu m$ and the $200\,\mu m$ core fibres, respectively. The spatial profiles of the back-propagated ultrasound fields were in good agreement with the optical fibre diameters, with FWHMs of $125\,\mu m$ and $195\,\mu m$ for the $105\,\mu m$-core and $200\,\mu m$-core fibres, respectively. Side lobes were visible in the back-propagated maximum pressure profiles (Figures 3(c) and 3(f)). Examination of the temporal profiles of the back-propagated waves revealed that the side lobes corresponded to ultrasound waves propagating laterally from the fibre end faces (data not shown).
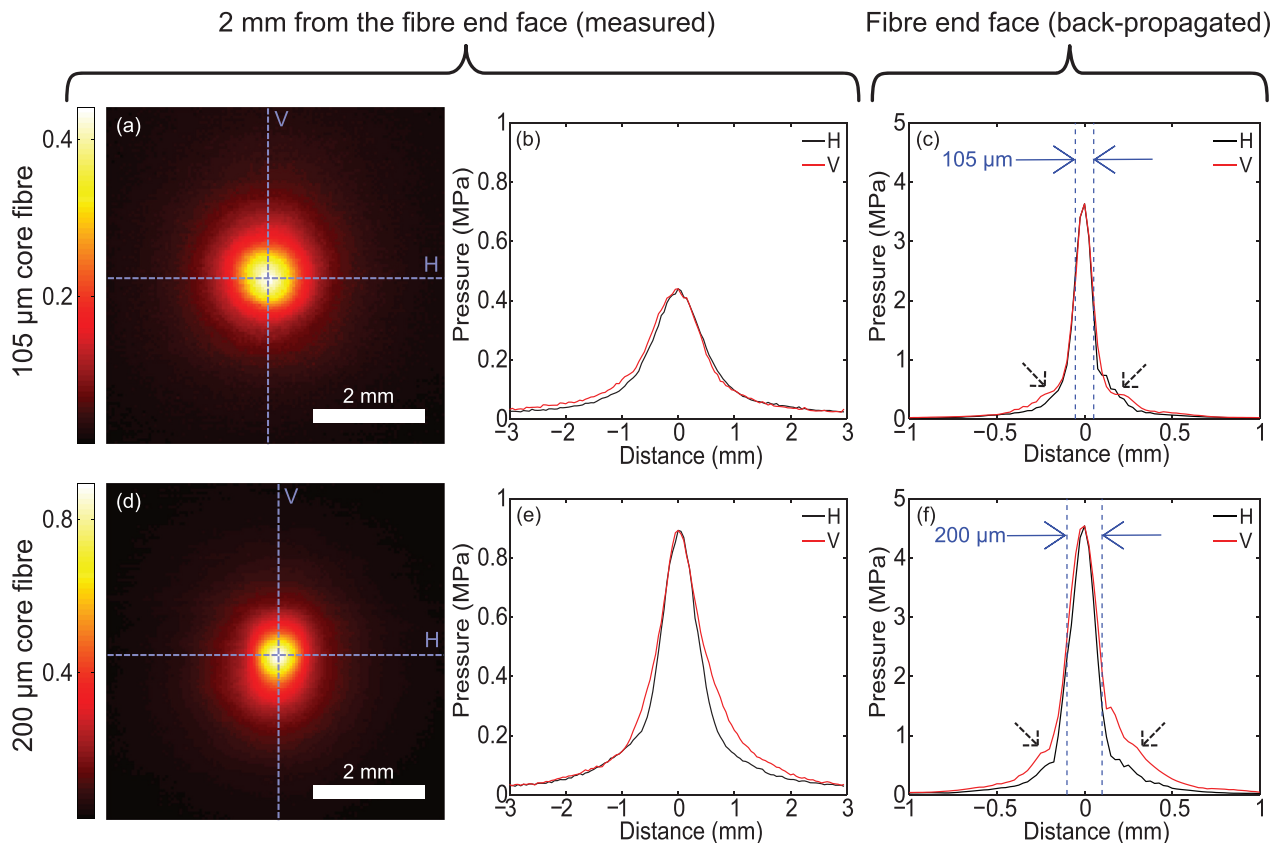

FIG. 3. (a) Peak ultrasound pressures measured in a plane 2 mm from the end face of the $105\,\mu m$-core diameter optical fibre. (b) Horizontal (H) and vertical (V) cross-sections of the pressures shown in (a). (c) Peak ultrasound pressures in the plane coincident with to the optical fibre end face, as calculated with back-propagation from measurements (side lobes indicated with black dashed arrows). (d)–(f) Corresponding measurements and calculations for the $200\,\mu m$-core diameter optical fibre.
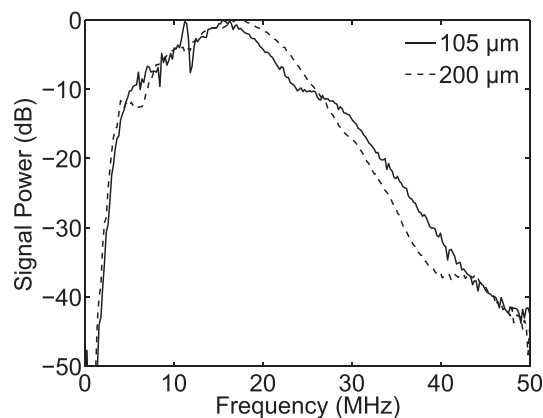
FIG. 4. Power spectra of the ultrasound pulses generated from the optical fibres with maximum pressures referenced to 0 dB.

The power spectra were similar for both optical fibre diameters (Figure 4). From the optical fibres with core diameters of 105 μm and 200 μm, the peak frequencies were 16 MHz and 18 MHz, respectively. The -3 dB bandwidths were 8 MHz and 10 MHz; the -6 dB bandwidths were 12 MHz and 15 MHz.

The ultrasound pressures that were achieved in this study compare favourably with recently reported results. In the study of Tian *et al.*, a pressure amplitude of 2.73 kPa was achieved at a distance of 1.5 mm using a gold nanopore array on the end face of a 62.5 μm core optical fibre.[17] In the study of Baac *et al.*,[18] a peak positive pressure of 22 MPa was measured at the focus of an optical ultrasound transducer that comprised a CNT-PDMS composite on a concave surface 6 mm in diameter and with a fluence of 42.4 mJ/cm^2. While this pressure was 4.9 times higher than that achieved in this study, it was produced using an effective focal gain of 54.

The ultrasound pressures and bandwidths of the generated ultrasound were consistent with those used for intravascular ultrasound.[1] Given that the instantaneous ultrasound pulse pressure is proportional to the temporal derivative of the corresponding light pulse in ideal conditions,[19] and that each light pulse was only 2 ns in duration, it is likely that the ultrasound bandwidth could be increased. Previous studies highlighted the need for thin coatings due to attenuation of high frequencies within the composite.[10] Thinner coatings might be achieved with a decrease in the withdrawal speed during dip coating[12] or with an increase in the xylene concentration to reduce the viscosity. However, a decrease in the coating thickness is likely to decrease the optical absorption and the corresponding ultrasound pressure. To compensate, the CNT concentration could be increased, but this might decrease the thermal expansion coefficient of the coating or result in a weaker adhesion between the coating and the optical fibre. A computational model that incorporates both optical and mechanical properties of the coating may be beneficial to estimate parameters for particular optimisation criteria.

The method for creating and applying composite coatings could be extended in several ways. For instance, functionalisation could be applied to carbon nanostructures distinct from CNTs, such as carbon black or graphene, to enhance their solubility in organic solvents of PDMS. Additionally, the dipping solutions might be readily applied to substrates distinct from optical fibres using spin coating. To coat optical fibres, functionalisation may not be required if carbon nanostructures are first deposited or grown onto the end faces and dip coating is used to overlay thin layers of pure PDMS.

In conclusion, this study demonstrated that uniform CNT-PDMS composite coatings for optical ultrasound generation can be created by functionalising the CNTs and then dissolving them into an organic PDMS solvent, and that coatings can be applied to optical fibre end faces using dip coating. The optical transducers created with these CNT-PDMS composite coatings have strong potential to be viable alternatives to electrical transducers, and they may offer significant advantages in terms of simplicity of fabrication and ease of integration into medical imaging probes.

[1]S. E. Nissen and P. Yock, Circulation **103**, 604 (2001).
[2]X. Li, W. Wu, Y. Chung, W. Y. Shih, W.-H. Shih, Q. Zhou, and K. K. Shung, IEEE Trans. Ultrason. Ferroelectr. Freq. Control **58**, 2281 (2011).
[3]F. L. Degertekin, R. O. Guldiken, and M. Karaman, IEEE Trans. Ultrason. Ferroelectr. Freq. Control **53**, 474 (2006).
[4]B. T. Cox and P. C. Beard, J. Acoust. Soc. Am. **117**, 3616 (2005).
[5]Y. Hou, J.-S. Kim, S. Ashkenazi, S.-W. Huang, L. J. Guo, and M. O'Donnell, Appl. Phys. Lett. **91**, 073507 (2007).
[6]T. Buma, M. Spisar, and M. O'Donnell, Appl. Phys. Lett. **79**, 548 (2001).
[7]A. Acquafresca, E. Biagi, L. Masotti, and D. Menichelli, IEEE Trans. Ultrason. Ferroelectr. Freq. Control **50**, 1325 (2003).
[8]C. I. Swift, S. G. Pierce, and B. Culshaw, Electron. Lett. **36**, 2113 (2000).
[9]S. H. Lee, M. Park, J. J. Yoh, H. Song, E. Y. Jang, Y. H. Kim, S. Kang, and Y. S. Yoon, Appl. Phys. Lett. **101**, 241909 (2012).
[10]H. W. Baac, J. G. Ok, H. J. Park, T. Ling, S.-L. Chen, A. J. Hart, and L. J. Guo, Appl. Phys. Lett. **97**, 234104 (2010).
[11]D. J. Lipomi, R. V. Martinez, M. A. Kats, S. H. Kang, P. Kim, J. Aizenberg, F. Capasso, and G. M. Whitesides, Nano Lett. **11**, 632 (2011).
[12]M. Kuroda and T. Nishino, Rev. Sci. Instrum. **82**, 063707 (2011).
[13]S. Majeed, V. Filiz, S. Shishatskiy, J. Wind, C. Abetz, and V. Abetz, Nanoscale Res. Lett. **7**, 296 (2012).
[14]J. C. Bear, P. D. McNaughter, K. Jurkschat, A. Crossley, L. Aldous, R. G. Compton, A. G. Mayes, and G. G. Wildgoose, J. Colloid Interface Sci. **383**, 110 (2012).
[15]B. E. Treeby and B. T. Cox, J. Biomed. Opt. **15**, 021314 (2010).
[16]B. E. Treeby, J. Jaros, A. P. Rendell, and B. T. Cox, J. Acoust. Soc. Am. **131**, 4324 (2012).
[17]Y. Tian, N. Wu, X. Zou, H. Felemban, C. Cao, and X. Wang, Opt. Eng. **52**, 065005 (2013).
[18]H. W. Baac, J. G. Ok, A. Maxwell, K.-T. Lee, Y.-C. Chen, A. J. Hart, Z. Xu, E. Yoon, and L. J. Guo, Sci. Rep. **2**, 989 (2012).
[19]D. Menichelli and E. Biagi, J. Opt. A: Pure Appl. Opt. **3**, S23 (2001).